Theoretical Investigation on the $GaCl_3$-Catalyzed Ring-Closing Metathesis Reaction of *N*-2,3-Butadienyl-2-propynyl-1-amine: Three-Membered Ring versus Four-Membered Ring Mechanism†

Yuanqiang Zhu and Yong Guo*

Department of Chemistry, Sichuan University, Chengdu 610064, China

Daiqian Xie*

Institute of Theoretical and Computational Chemistry, Key Laboratory of Mesoscopic Chemistry, School of Chemistry and Chemical Engineering, Nanjing 210093, China

Received: May 22, 2007; In Final Form: August 2, 2007

The gallium chloride ($GaCl_3$)-catalyzed ring-closing metathesis reaction mechanism of *N*-2,3-butadienyl-2-propynyl-1-amine has been studied at the Becke three-parameter hybrid functional combined with Lee−Yang−Parr correlation functional (B3LYP)/6-31G(d), B3LYP/6-31+G(d,p), B3LYP/6-311++G(d,p)//B3LYP/6-31G(d) and the second-order Møller-Plesset perturbation (MP2)/6-311++G(d,p)//B3LYP/6-31+G(d,p) levels. It was found that the final metathesis product can be yielded via a three-membered or four-membered ring mechanism. The three-membered ring pathway is favorable due to its low energy barrier at the rate determining step. The whole reaction is stepwise and strongly exothermic.

1. Introduction

Lewis-acid catalysts are known to be able to enhance the reaction rates and endo selectivities of Diels−Alder reactions.[1−4] $GaCl_3$, known as a group 13 Lewis acid, has been for a long time considered to be analogous to $AlCl_3$ but with lower reactivity. Recent studies, however, have revealed that $GaCl_3$ exhibits novel properties in organic synthesis, whereas $AlCl_3$ does not.[5,6] More recently, $GaCl_3$ has been used as a good activator in many organic reactions, especially for alkynes, benzene, and enynes.[7−15]

In 2002, Chatani and co-workers[16] reported the skeletal reorganization of enynes catalyzed by $GaCl_3$. They believed that the mechanism involves the production of the cyclobutene ring, cyclobutane ring, and three-center two-electron bond intermediates (Figure 1). The ring opening of both cyclobutene and cyclobutane rings would lead to the product.[17] The electrophilic addition of $GaCl_3$ to an acetylene affords the vinyl-gallium species,[18] which can be stabilized by the olefinic portion.[19] Recently, Kim and co-workers[20] discovered that a treatment of enyne with $GaCl_3$ can afford an eight-membered ring compound in high yields, which was different from the mechanism proposed by Mehta and Singh.[21] They believed that the plausible mechanism is similar to the one suggested by Chatani's group except without the corresponding three-center two-electron bond intermediate.[16] Some studies showed that $GaCl_3$ is an extremely active catalyst for the skeletal rearrangement of 1,6-enynes and 1,7-enynes.[22−24] Lee and co-workers[25] studied the cycloisomerization of allenynes with $GaCl_3$ or $[Au(PPh_3)]SbF_6$ as a catalyst and isolated the metathesis product with high yields. The cycloisomerized product was the same type as those generated from the molybdenum alkylidene complex catalyzed ring-closing metathesis of allenynes,[26] while different from those obtained from $PtCl_2$-catalyzed cycloisomerization of allenynes.[27,28] They further examined several other metathesis reactions of allenynes catalyzed by $GaCl_3$ and Au(I). From their experimental observations, they suggested that the mechanism would follow the general process (Figure 2),[22−24] but different from that proposed by Murakami,[26] who considered that the mechanism involves several four-membered rings formed by transition metal molybdenum.

There have been some theoretical studies on the mechanisms of the $GaCl_3$-catalyzed reactions.[29−34] However, to our best knowledge, a general mechanistic view for the $GaCl_3$ catalyzed ring-closing metathesis reaction of allenynes has so far remained elusive. The motive of the present study is to clarify the mechanism of the ring-closing metathesis reaction of *N*-2,3-butadienyl-2-propynyl-1-amine and to make it clear that $GaCl_3$ is desirable for the detachment from the product. In the present study, we have performed detailed calculations using the B3LYP hybrid functional method to study the title reaction. In addition, we have carried out the natural bond orbital (NBO) analysis to investigate the bond order changes.

2. Computational Details

All calculations were carried out with the Gaussian 03 program.[35] Since the real reaction system is too huge for precise calculations, we studied a model system as shown in Figure 3. As the substituent groups merely play a minor role in the reaction process, it is expected that the reactivity for the model system should be very similar to that of the real system. The DFT calculations at the B3LYP[36,37]/6-31G(d) and B3LYP/6-31+G(d,p) levels were used to optimize the stationary points in the reaction process. For each stationary point on the potential energy surface, a frequency calculation was carried out to generate its thermal correction to the Gibbs free energy and to verify whether it is a minimum or a transition state. Single-

† Part of the "Sheng Hsien Lin Festschrift".

* To whom correspondence should be addressed. E-mail: dqxie@nju.edu.cn (D.X.); 163guoyong@163.com (Y.G.).

10.1021/jp073939g CCC: $37.00
Published on Web 08/21/2007

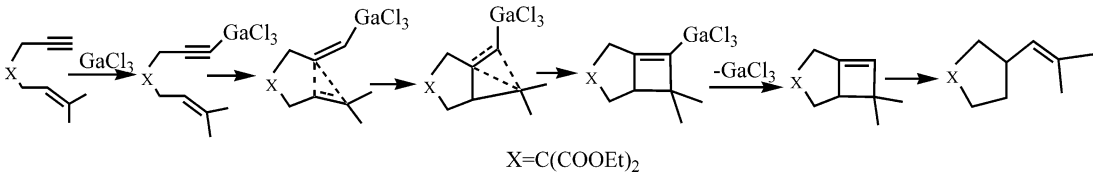

Figure 1. Possible skeletal reorganization mechanism of enynes catalyzed by $GaCl_3$.

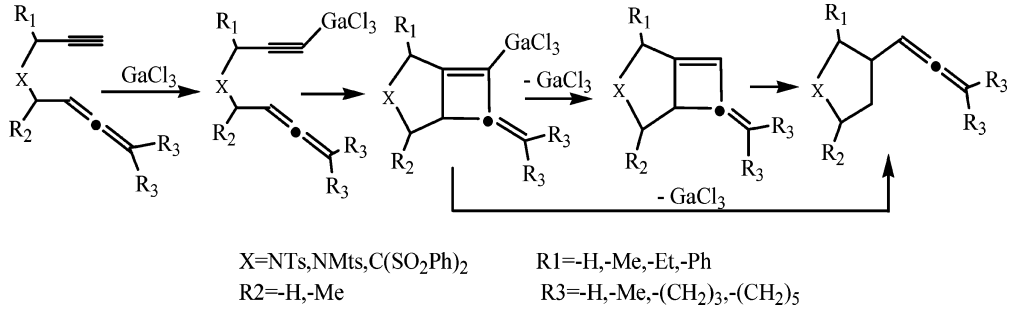

Figure 2. Possible four-member-ring mechanism of $GaCl_3$-catalyzed allenyne cycloisomerization to allenene.

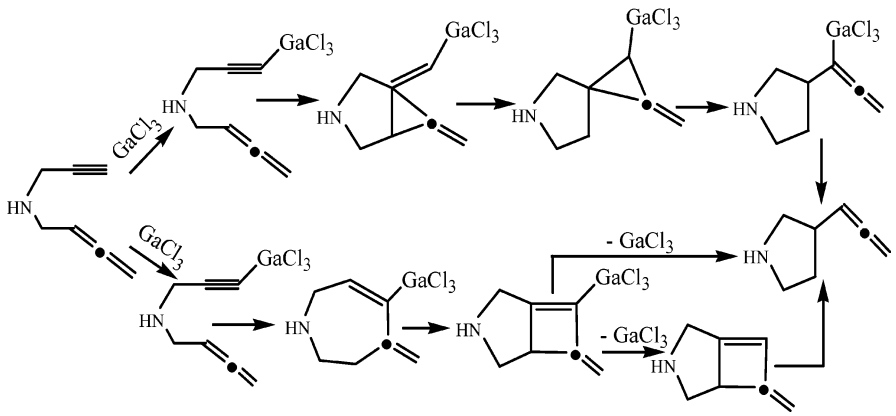

Figure 3. Two reaction pathways in the modeled reaction system.

point energy calculations were carried out at the B3LYP/6-311++G(d,p)//B3LYP/6-31G(d) and MP2/6-311++G(d,p)//B3LYP/6-31+G(d,p) levels. In order to further confirm the breaking and forming of chemical bonds, the electronic structures of stationary points were analyzed by the natural bond orbital (NBO) method.[38] In the following, the reported energy barriers were calculated by comparing the free energies of the transition states with those of the corresponding intermediates. All relative energies include the thermal corrections.

3. Results and Discussions

3.1. Three-Membered Ring Mechanism. The corresponding structures and atomic labels of the stationary points are depicted in Figure 4 together with the important bond lengths and the Wiberg bond index. The calculated relative energies and the potential energy profile are presented in Figure 5. Since different calculation levels show the same tendency for the title reaction, in the following sections, we will focus on the geometries and Wiberg bond indices obtained at the B3LYP/6-31G(d) level and the energies obtained at the B3LYP/6-311++G(d,p)//B3LYP/6-31G(d) level. As shown in Figure 5, this pathway proceeds via five steps. The first step is the coupling of the catalyst $GaCl_3$ with reactant **R**. The fifth step is the direct detachment of $GaCl_3$ from final product **P**. For **R**, one can see from Figure 4 that the C6−C7, C9−C11, and C11−C12 bond distances are 1.2070, 1.3079, and 1.3064 Å, respectively, and the corresponding Wiberg bond indices are 2.8958, 1.9209, and 1.9855, respectively. It is obvious that the C6−C7 bond has the nature of a triple bond and the C9−C11 and C11−C12 bonds are characterized with the nature of a double bond. In the first step, the catalyst couples with the C6−C7 triple bond to give an intermediate **IM1** without energy barrier. In **IM1**, the C7−Ga17 bond distance is 2.3069 Å and the Wiberg bond index is 0.2208, which shows that the C7−Ga17 bond is only partly formed. It is the coupling that leads to the lengthening of the C6−C7 bond distance to 1.2242 Å and to the decrease of the Wiberg bond index to 2.6530. As shown in Figure 5, the coupling decreases the free energy of the system slightly by 1.25 kcal/mol at the B3LYP/6-311++G(d,p) level. The electrophilic addition of $GaCl_3$ to *N*-2,3-butadienyl-2-propynyl-1-amine produces the vinyl-gallium species, **IM1**, which is stabilized by the olefinic portion.

In the second step, the carbon atoms C9 and C11 synchronously attack the carbon atom C6 to give an intermediate **IM2** through a three-membered ring transition state **TS1**. The imaginary frequency of **TS1** is 236.46i cm^{-1}. An analysis of the vibrational modes indicates that **TS1** connects exactly with **IM1** and **IM2**. In **IM1**, the distance between the C11 and the C6 atoms is larger than 3.0 Å, whereas in **TS1**, as shown in Figure 4, the C6−C9 and the C6−C11 bond distances shorten to 2.1641 and 2.2800 Å, respectively. Thus, the corresponding Wiberg bond indices increase to 0.2701 and 0.1972, respectively. In **IM2**, the two bond distances further shorten to 1.5711 and 1.6284 Å, and the Wiberg bond indices increase to 0.8197 and 0.6338. Meanwhile, the C9−C11 bond length increase from 1.3086 Å in **IM1** to 1.4236 Å in **IM2**. These changes of the

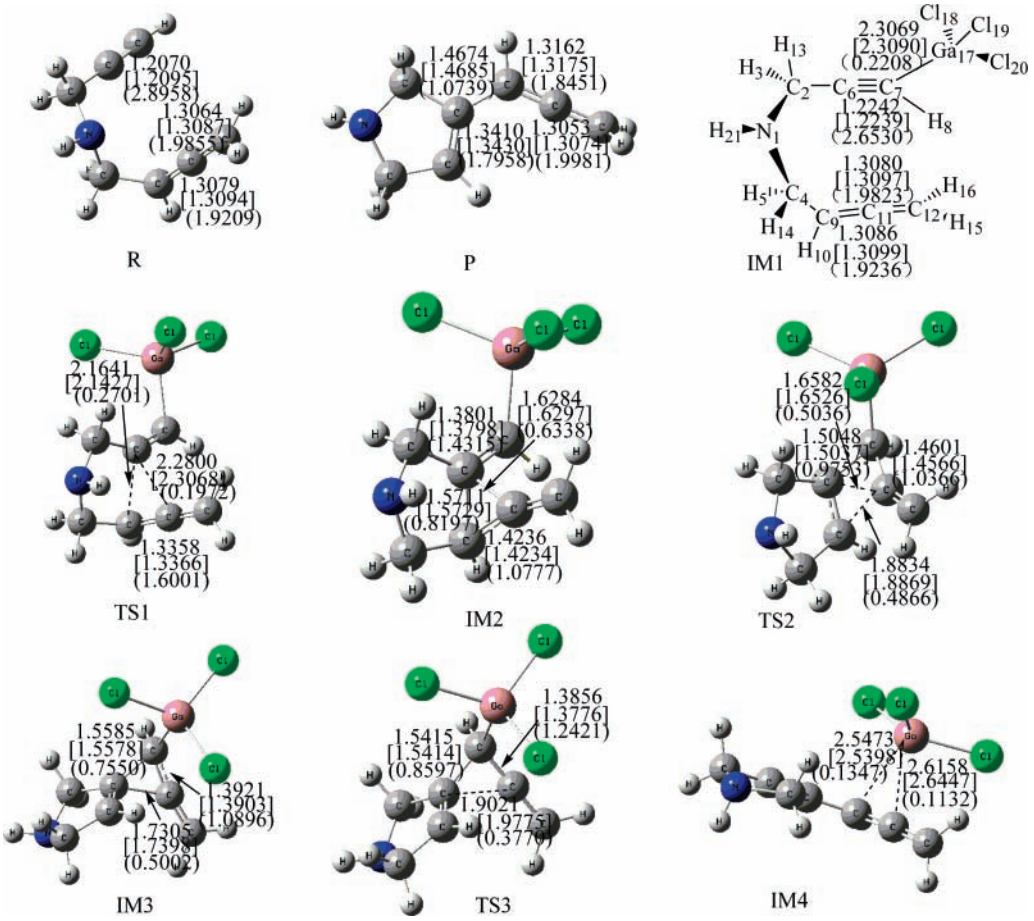

Figure 4. Optimized geometries of the three-membered ring pathway of the $GaCl_3$-catalyzed reaction of *N*-2,3-butadienyl-2-propynyl-1-amine at the B3LYP/6-31G(d) (without brackets) and B3LYP/6-31+G(d,p) (in square brackets) levels (bond distance in Å; numbering atom seeing **IM1**) and the Wiberg bond indices at the B3LYP/6-31G(d) (in round brackets) level.

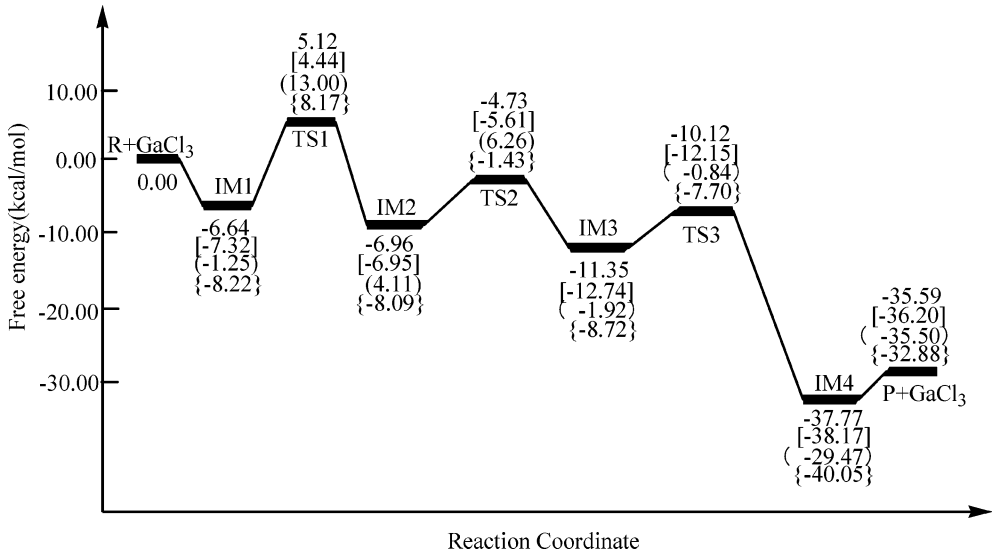

Figure 5. Schematic potential energy profile of the three-membered ring pathway for the title reaction at the B3LYP/6-31G(d) (without brackets), B3LYP/6-31+G(d,p) (in square brackets), B3LYP/6-311++G(d,p)//B3LYP/6-31G(d) (in round brackets), and MP2/6-311++G(d,p)//B3LYP/6-31+G(d,p) (in big brackets) levels.

bond distances and the Wiberg bond indices indicate that the three-membered ring intermediate **IM2** is to be formed through the forming of the C6−C9 and C6−C11 bonds and the lengthening of the C9−C11 bond. Our calculated results show that the free energy barrier is 14.25 kcal/mol at the B3LYP/6-311++G(d,p) level. From Figure 4, one can also see that a three-center two-electron bond is involved in **IM2**, which is consistent with the intermediate proposed by Chatani' group.[16]

In the third step, the carbon atom C11 was transferred to the carbon atom C7 to produce another three-membered ring intermediate **IM3** through a transition state **TS2**. In **TS2**, the C6−C11 bond distance is 1.6582 Å, which is 0.0298 Å longer

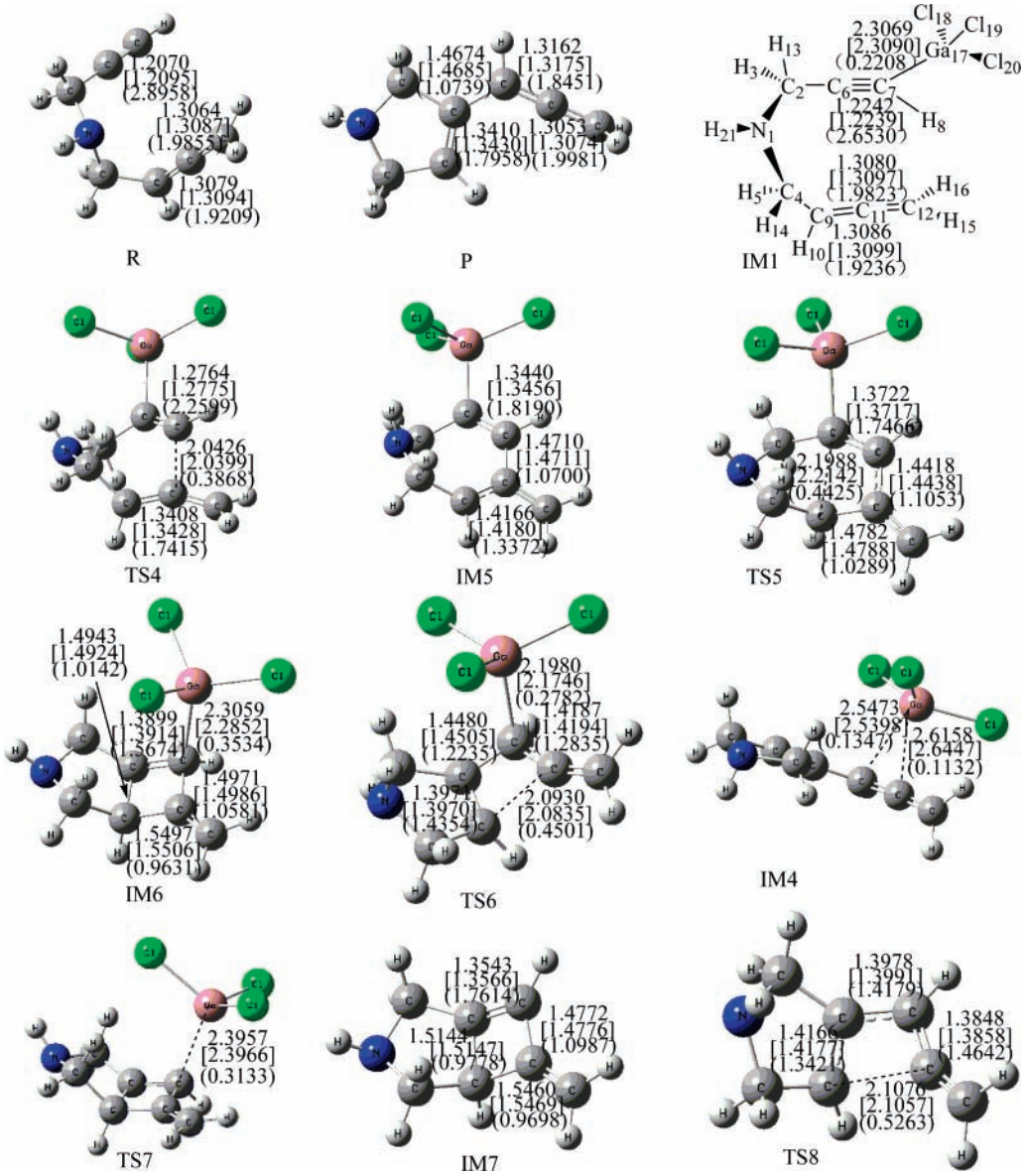

Figure 6. Optimized geometries of the four-membered ring pathway of $GaCl_3$-catalyzed reaction of *N*-2,3-butadienyl-2-propynyl-1-amine at the B3LYP/6-31G(d) (without brackets) and B3LYP/6-31+G(d,p) (in square brackets) levels (bond distance in Å; numbering atom seeing IM1) and the Wiberg bond indices at the B3LYP/6-31G(d) (in round brackets) level.

than that in **IM2**, and the Wiberg bond index is 0.5036, which is 0.1302 smaller than that in **IM2**. The C9−C11 bond distance is 0.4598 Å longer than that in **IM2**, and the corresponding Wiberg bond index is 0.5911 smaller than that in **IM2**. In **IM3**, the C6−C11 bond distance is 1.7305 Å, which is 0.0723 Å longer than that in **TS2**, and the Wiberg bond index is 0.5002, which is 0.0034 smaller than that in **TS2**. Although the C6−C11 bond distance becomes longer, the Wiberg bond index indicates that this bond is only partly broken. The C9−C11 bond is broken with a bond distance of 2.5111 Å in **IM3**. Thus, **IM3** is still a three-membered ring intermediate. The formation of the intermediate **IM3** needs to surmount only a low-energy barrier of 2.15 kcal/mol.

In the fourth step, the intermediate **IM3** affords an intermediate **IM4** through a three-membered ring transition state **TS3** by breaking the C6−C11 bond. **TS3** has only one imaginary frequency, the vibrational mode of which is exactly associated with the stretching motion of the C6−C11 bond. In **TS3**, the C6−C11 bond distance is 0.1716 Å longer than that in **IM3**, and the corresponding Wiberg bond index is 0.1232 smaller than that in **IM3**. The C7−C11 bond distance is 1.3856 Å, which is 0.0065 Å shorter than that in **IM3**, and the corresponding Wiberg bond index is 1.2421, which is 0.1561 larger than that in **IM3**. One can see that **TS3** has the tendency to afford **IM4**. With the breaking of the C6−C11 bond, the intermediate **IM4** is formed. In **IM4**, the C6−C11 bond distance is 2.4756 Å, which indicates the complete breaking of the bond. As shown in Figure 5, the breaking of the C6−C11 bond needs a free energy barrier of 1.08 kcal/mol only. Moreover, **IM4** is more stabilization than IM3 with stabilization energy of about 30 kcal/mol.

In the final step, the intermediate **IM4** yields the final product **P** through a direct detachment of the catalyst $GaCl_3$ without energy barrier. In **IM4**, the C7−Ga17 and C11−Ga17 bonds distances are 2.5473 and 2.6158 Å, and the Wiberg bond indices are 0.1347 and 0.1132, respectively. The large bond distances and small Wiberg bond indices show that the catalyst $GaCl_3$ is desirable for the detachment from the final product. In the final product, the Wiberg bond indices of the C7−C11 and C11−C12 bonds are 1.8451 and 1.9981, respectively, which characterize the nature of a double bond. According to the reaction processes, one can see that the carbon atom C11 moves from

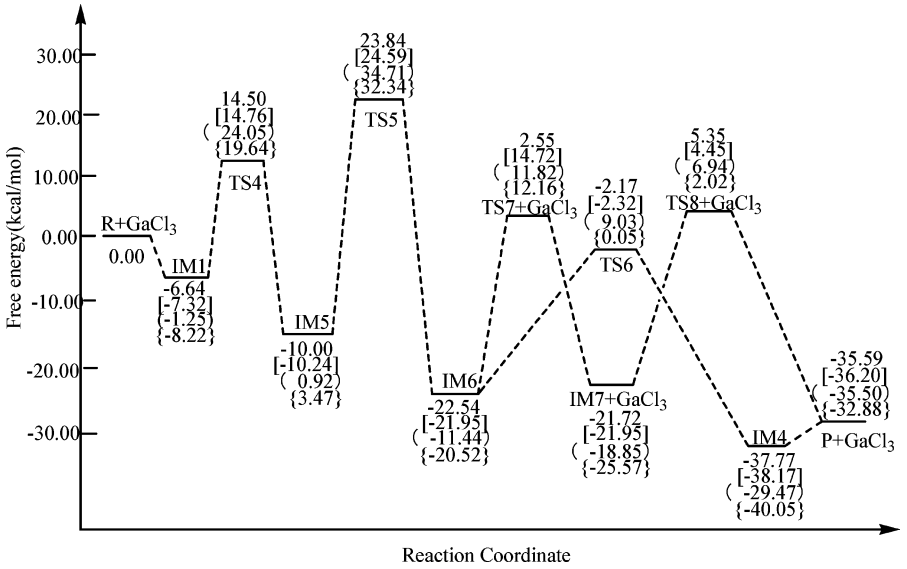

Figure 7. Schematic potential energy profile of the four-membered ring pathway for the title reaction at the B3LYP/6-31G(d) (without brackets), B3LYP/6-31+G(d,p) (in square brackets), B3LYP/6-311++G(d,p)//B3LYP/6-31G(d) (in round brackets) and MP2/6-311++G(d,p)//B3LYP/6-31+G(d,p) (in big brackets) levels.

the carbon atom C9 in the reactant to the carbon atom C7 in the final product. Therefore, the whole process is a ring-closing metathesis reaction.

Although Chatani and co-workers[16] have proposed the three-center two-electron bond intermediate, they did not give the corresponding three-membered ring mechanism. As shown in Figure 5, the formation of **IM2** is the rate-determining step with an energy barrier of 14.25 kcal/mol. In addition, the free energy of the product is much lower than that of the reactant. As a result, this reaction can easily proceed with the catalyst $GaCl_3$.

3.2. Four-Membered Ring Mechanism. The corresponding structures, atom labels, important bond lengths, and Wiberg bond indices of the stationary points are depicted in Figure 6. The calculated relative energies and the potential energy profile are presented in Figure 7. The first step is the same as that in the three-membered ring pathway.

In the second step, the C11 atom attacks the C7 atom to form an intermediate **IM5** through a transition state **TS4**. The imaginary frequency of **TS4** is 477.47i cm^{-1}. An analysis of the vibrational modes indicates that this imaginary frequency is exactly associated with the C7−C11 bond stretching motion. Clearly, **TS4** connects correctly with **IM1** and **IM5**. In **TS4**, the C7−C11 bond distance is 2.0426 Å, and the Wiberg bond index is 0.3868, whereas in **IM5**, the bond distance shortens to 1.4710 Å, and the corresponding Wiberg bond index increases to 1.0700. It is obvious that the C7−C11 bond is being formed during this step. The formation of the C7−C11 bond needs to surmount a barrier height of 25.30 kcal/mol.

In the third step, the C9 atom attacks the C6 atom to form the four-membered ring intermediate **IM6** through a transition state **TS5**. In **TS5**, the C6−C9 bond distance is 2.1988 Å, and the Wiberg bond index is 1.4425. With the formation of the C6−C9 bond, **IM6** is generated with a stabilization energy of 22.54 kcal/mol. In **IM6**, the bond distance shortens to 1.4943 Å, and the corresponding Wiberg bond index increases to 1.0142. The formation of the C6−C9 bond needs an activation free energy of 33.79 kcal/mol. **IM6** is a cyclobutane ring intermediate, which is consistent with the results reported by Lee and co-workers.[25]

As suggested by Lee and co-workers,[18] **IM6** yields the final product through two different reaction pathways. In one pathway, the **IM6** affords **IM4** through a transition state **TS6** by breaking of the C9−C11 bond. In **TS6**, the C9−C11 bond distance is 2.0930 Å, which is 0.5433 Å longer than that in **IM6**, and the Wiberg bond index is 0.4501, which is 0.5130 smaller than that in **IM6**. In **IM4**, the C9−C11 bond is completely broken with a bond distance of 2.4756 Å. After surmounting **TS6** with a free energy barrier of 20.47 kcal/mol, **IM4** is generated. Then **IM4** directly undergoes a detachment of $GaCl_3$ to yield the final product. In another pathway, an intermediate **IM7** is generated through the detachment of the catalyst $GaCl_3$ from **IM6** through a transition state **TS7** with a free energy barrier height of 23.26 kcal/mol. In **TS7**, the C7−Ga17 bond distance is 2.3957 Å, which is 0.0898 Å longer than that in **IM6**, and the corresponding Wiberg bond index is 0.3133, which is 0.0401 smaller than that in **IM6**. The Wiberg bond indices show that the transition state **TS7** is a reactant-like geometry due to the small differences between **TS7** and **IM6**. **IM7** is a cyclobutene ring intermediate, which is consistent with the results reported by Lee and co-workers.[18] Subsequently, **IM7** affords the final product through a transition state **TS8** by breaking of the C9−C11 bond. In **TS8**, the C9−C11 bond distance is 0.5616 Å longer than that in **IM7**, and the Wiberg bond index is 0.4435 smaller than that in **IM7**. These changes indicate the gradual breaking of the C9−C11 bond and the yield of the product. In the final product, the C11 atom moves completely from C9 to C7 atom. Accordingly, this pathway is a ring-closing metathesis mechanism. As shown in Figure 7, the transformation from **IM7** into **P** needs to surmount a free energy barrier of 25.79 kcal/mol. Between the two different pathways, the first one via **TS6** is favorable due to its lower free energy barrier, which is in good agreement with the mechanism reported by Lee and co-workers.[25]

With the formation of the final product, the four-membered ring pathway is completely accomplished. In this pathway, as shown in Figure 7, the formation of the **IM6** is the rate-determining step with a free energy barrier of 33.79 kcal/mol.

As shown in Figures 5 and 7, the rate determining step of the three-membered ring pathway has a much lower activation free energy than that of the four-membered ring pathway. Therefore, the three-membered ring pathway is favorable. In addition, the free energy of the product is much lower than that

of the reactant. As a result, this reaction can be easily carried out with the catalyst $GaCl_3$.

4. Conclusions

The $GaCl_3$-catalyzed ring-closing metathesis reaction mechanism of *N*-2,3-butadienyl-2-propynyl-1-amine has been investigated at the B3LYP/6-31G(d), B3LYP/6-31+G(d,p), and B3LYP/6-311++G(d,p)//B3LYP/6-31G(d), MP2/6-311++G(d,p)// B3LYP/6-31+G(d,p) levels. The reaction may proceed via two possible pathways. The three-membered ring pathway is favorable due to its lower activation free energy. Furthermore, the free energy of the product is much lower than that of the reactant. As a result, this reaction can be easily carried out under the existence of the catalyst $GaCl_3$. In addition, the detachment of the catalyst $GaCl_3$ is desirable for the substrate. The detailed mechanism of the reaction should provide useful information for further studies.

Acknowledgment. This work was supported by the National Natural Science Foundation of China (Grant Nos. 10574068 and 20533060) and by the Sichuan Applied Fundamental Research Project.

Supporting Information Available: The optimized geometries and standard Cartesian coordinates of all stationary points. This material is available free of charge via the Internet at http://pubs.acs.org.

References and Notes

(1) Yates, P.; Eaton, P. *J. Am. Chem. Soc.* **1960**, *82*, 4436.
(2) Inukai, T.; Kojima, T. *J. Org. Chem.* **1971**, *36*, 924.
(3) Chen, Z.; Ortuño, R. M. *Tetrahedron*: *Asymmetry.* **1994**, *5*, 371.
(4) Maruoka, K.; Asakura, M.; Saitoh, S.; Ooi, T.; Yamamoto, H. *J. Am. Chem. Soc.* **1994**, *116*, 6153.
(5) Yamaguchi, M. In *Science of Synthesis*, *Houben-Weyl*, *Methods of Molecular Transformations*; Noyori, R., Yamamoto, H., Eds.; Georg Thieme Verlag: Stuttgart, 2004; Vol. 7, pp 387−412.
(6) Yamaguchi, M. In *Main Group Metals in Organic Synthesis*; Yamamoto, H., Oshima, K., Eds.; Wiley-VCH Verlag: Weinheim, Germany, 2004; pp 307−322.
(7) Kido, Y.; Yoshimura, S.; Yamaguchi, M.; Uchimaru, T. *Bull. Chem. Soc. Jpn.* **1999**, *72*, 1445.
(8) Arisawa, M.; Miyagawa, C.; Yoshimura, S.; Kido, Y.; Yamaguchi, M. *Chem. Lett*. **2001**, 1080.
(9) Asao, N.; Asano, T.; Ohishi, T.; Yamamoto, Y. *J. Am. Chem. Soc*. **2000**, *122*, 4817.
(10) Kobayashi, K.; Arisawa, M.; Yamaguchi, M. *J. Am. Chem. Soc.* **2002**, *124*, 8528.
(11) Viswanathan, G. S.; Wang, M.; Li, C.-J. *Angew. Chem., Int. Ed*. **2002**, *41*, 2138.
(12) Yonehara, F.; Kido, Y.; Morita, S.; Yamaguchi, M. *J. Am. Chem. Soc.* **2001**, *123*, 11310.
(13) Kido, Y.; Yonehara, F.; Yamaguchi, M. *Tetrahedron* **2001**, *57*, 827.
(14) Arisawa, M.; Akamatsu, K.; Yamaguchi, M. *Org. Lett.* **2001**, *3*, 789.
(15) Arisawa, M.; Amemiya, R.; Yamaguchi, M. *Org. Lett.* **2002**, *4*, 2209.
(16) Chatani, N.; Inoue, H.; Kotsuma, T.; Murai, S. *J. Am. Chem. Soc.* **2002**, *124*, 10294.
(17) Fürstner, A.; Stelzer, F.; Szillat, H. *J. Am. Chem. Soc*. **2001**, *123*, 11863.
(18) Inoue, H.; Chatani, N.; Murai, S. *J. Org. Chem*. **2002**, *67*, 1414.
(19) Méndez, M.; Munõz, M. P.; Nevado, C.; Ca'rdenas, D. J.; Echavarren, A. M. *J. Am. Chem. Soc*. **2001**, *123*, 10511.
(20) Kim, S. M.; Lee, S. I.; Chung, Y. K. *Org. Lett.* **2006**, *8*, 5425.
(21) Mehta, G.; Singh, V. *Chem. Rev.* **1999**, *99*, 881.
(22) Mamane, V.; Hannen, P.; Fûrstner, A. *Chem. Eur. J*. **2004**, *10*, 4556.
(23) Chatani, N.; Oshita, M.; Tobisu, M.; Ishii, Y.; Murai, S. *J. Am. Chem. Soc*. **2003**, *125*, 7812.
(24) Fûrstner, A.; Mamane, V. *J. Org. Chem*. **2002**, *67*, 6264.
(25) Lee, S. I.; Sim, S. H.; Kim, S. M.; Kim, K.; Chung, Y. K. *J. Org. Chem.* **2006**, *71*, 7120.
(26) Murakami, M.; Kadowaki, S.; Matsuda, T. *Org. Lett*. **2005**, *7*, 3953.
(27) Matsuda, T.; Kadowaki, S.; Goya, T.; Murakami, M. *Synlett* **2006**, *4*, 575.
(28) Cadran, N.; Cariou, K.; Hervé, G.; Aubert, C.; Fensterbank, L.; Malacria, M.; Marco-Contelles, J. *J. Am. Chem. Soc*. **2004**, *126*, 3408.
(29) Wu, Y.; Xu, K. L.; Xie, D. Q. *Tetrahedron* **2005**, *61*, 507.
(30) Yamabe, S.; Minato, T. *J. Org. Chem.* **2000**, *65*, 1830.
(31) Wong, C. T.; Wong, M. W. *J. Org. Chem.* **2007**, *72*, 1425.
(32) Volkov, A. N.; Timoshkin, A. Y.; Suvorov, A. V. *Int. J. Quantum Chem.* **2005**, *104*, 256.
(33) Villinger, A.; Mayer, P.; Schulz, A. *Chem. Comm.* **2006**, *11*, 1236.
(34) Xu, K. L.; Wu, Y.; Xie, D. Q.; Yan, G. S. *Chin. Sci. Bull*. **2004**, *49*, 883.
(35) Frisch, M. J.; Trucks, G. W.; Schlegel, H. B.; Scuseria, G. E.; Robb, M. A.; Cheeseman, J. R.; Montgomery, J. A., Jr.; Vreven, T.; Kudin, K. N.; Burant, J. C.; Millam, J. M.; Iyengar, S. S.; Tomasi, J.; Barone, V.; Mennucci, B.; Cossi, M.; Scalmani, G.; Rega, N.; Petersson, G. A.; Nakatsuji, H.; Hada, M.; Ehara, M.; Toyota, K.; Fukuda, R.; Hasegawa, J.; Ishida, M.; Nakajima, T.; Honda, Y.; Kitao, O.; Nakai, H.; Klene, M.; Li, X.; Knox, J. E.; Hratchian, H. P.; Cross, J. B.; Bakken, V.; Adamo, C.; Jaramillo, J.; Gomperts, R.; Stratmann, R. E.; Yazyev, O.; Austin, A. J.; Cammi, R.; Pomelli, C.; Ochterski, J. W.; Ayala, P. Y.; Morokuma, K.; Voth, G. A.; Salvador, P.; Dannenberg, J. J.; Zakrzewski, V. G.; Dapprich, S.; Daniels, A. D.; Strain, M. C.; Farkas, O.; Malick, D. K.; Rabuck, A. D.; Raghavachari, K.; Foresman, J. B.; Ortiz, J. V.; Cui, Q.; Baboul, A. G.; Clifford, S.; Cioslowski, J.; Stefanov, B. B.; Liu, G.; Liashenko, A.; Piskorz, P.; Komaromi, I.; Martin, R. L.; Fox, D. J.; Keith, T.; Al-Laham, M. A.; Peng, C. Y.; Nanayakkara, A.; Challacombe, M.; Gill, P. M. W.; Johnson, B.; Chen, W.; Wong, M. W.; Gonzalez, C.; Pople, J. A. *Gaussian 03*, revision C.02; Gaussian, Inc.: Wallingford, CT, 2004.
(36) Becke, A. D. *J. Chem. Phys.* **1993**, *98*, 5648.
(37) Parr, R. G.; Yang, W. *Density-functional Theory of Atoms and Molecules*; Oxford University Press: Oxford, U.K., 1989.
(38) Reed, A. E.; Curtiss, L. A.; Weinhold, F. *Chem. Rev.* **1988**, *88*, 899.